The 2013 World Congress on
Advances in Structural Engineering and Mechanics (ASEM13)
Jeju, Korea, September 8-12, 2013

Gradient enhanced plasticity in engineering applications

*Somsak Swaddiwudhipong[1)], Zhishun Liu[2)], Xu-Dong Qian[3)]
and Leong-Hien Poh[3)]
[1), 3)] *Department of Civil and Environmental Engineering,*
National University of Singapore, Singapore 117576
[2)] *International Centre for Applied Mechnics, Xi'an Jiaotong University, PRC 710049*
[1)] *ceesomsa@nus.edu.sg*

ABSTRACT

Non-uniform plastic deformation of materials of small volume exhibits strong size dependence when deform at micro- and nano-metre levels. Classical continuum models also demonstrate strong mesh dependency during strain softening. A series of C^0 elements incorporating conventional mechanism-based strain gradient (CMSG) plasticity based on Taylor dislocation model and over-nonlocal gradient enhancement on damaged model have been established and implemented for engineering material applications. CMSG plasticity is incorporated to re-calibrate Weibull stress model for the prediction of fracture toughness probability distributions. Over-nonlocal gradient enhanced plasticity damage model is adopted to fully regularize the localized softening behavior of brittle materials in strain softening regime.

1. INTRODUCTION

Experiments carried out in the past few decades (Fleck et al, 1994, Stolken and Evans, 1998) demonstrated the strong size effects when the material length scale and non-uniform plastic deformation are of the same order at micron or submicron level. Classical continuum mechanics ceases to be valid at this range of deformation. Classical continuum models also demonstrate strong mesh dependency during material softening.

Huang et al. (2001) proposed the conventional theory of mechanism-based strain gradient (CMSG) plasticity obeying Taylor dislocation theory and yet preserving the classical continuum plasticity procedure. Swaddiwudhipong et al. (2005, 2006) adopted the CMSG plasticity model to establish a series of C^0 elements that can be implemented using classical finite element formulation. These CMSG solid elements have been employed in the computation of the near-tip stresses to evaluate the scalar microscopic crack driving force, the Weibull stress, σ_w for the re-calibration of the Weibull modulus, m, and the threshold fracture toughness, K_{min}.

An important aspect of concrete simulations is to study the material response until near failure state. Classical continuum models for softening materials are unable to provide meaningful post-peak results. Numerically, these models exhibit strong

[1) ,2)] Professor
[3)] Assistant Professor

pathological dependence on the orientation and size of the finite element mesh during strain softening. To the limit of infinitesimal element size, the softening behavior localizes to a set of zero volume and the material response approaches that of perfectly brittle behavior. A broad class of regularizing technique is the implicit gradient formulation where an additional Helmholtz equation is satisfied in a weak sense. However, standard gradient enhancement may not fully regularize the softening behavior for some models.

2. CMSG-BASED WEIBULL MODEL FOR CLEAVAGE FRACTURE ASSESSMENT

2.1 Weibull Stress Model

The Weibull stress framework, originally developed by Beremin (1983), has become a widely recognized approach to characterize the probability of brittle fracture failure for ferritic steels, which exhibit significant scatter in the measured fracture toughness over the ductile-to-brittle transition regime. The Weibull stress model couples the weakest link formulation with an inverse power law distribution of the microscopic flaws in the material. The probability of fracture follows,

$$P_f\left(\sigma_w\right) = 1 - \exp\left[-\left(\frac{\sigma_w}{\sigma_u}\right)^m\right], \tag{1}$$

where σ_u denotes an average stress representative of the micro-scale material fracture resistance and σ_w integrates the effective stress component (the maximum principal stress in this study) over the fracture process zone of a reference volume arbitrarily chosen as V_0,= 1 mm^3 herein, i.e.,

$$\sigma_w = \left[\frac{1}{V_0}\int_V \sigma_1^m dV\right]^{1/m}. \tag{2}$$

Wasiluk *et al*. (2006) extended the two-parameter Weibull stress model into a three-parameter Weibull stress model,

$$P_f\left(\sigma_w\right) = 1 - \exp\left[-\left(\frac{\sigma_w^{m/4} - \sigma_{min}^{m/4}}{\sigma_u^{m/4} - \sigma_{min}^{m/4}}\right)^4\right], \tag{3}$$

where σ_{min} defines the threshold Weibull stress, below which no cleavage fracture failure occurs. The parameter m, the Weibull modulus, characterizes the shape of the cumulative probability curve with respect to the microscopic crack driving force, σ_w. The three-parameter Weibull stress model matched successfully the macroscopic Weibull model based on the stress-intensity factor, which applies strictly to high-constraint, small-scale yielding laboratory fracture specimens (ASTM E-1921, 2012),

$$P_f = 1 - \exp\left[-\left(\frac{K_{Jc} - K_{min}}{K_0 - K_{min}} \right)^4 \right], \tag{4}$$

where K_{Jc} refers to the measured critical stress-intensity factor for a laboratory specimen, K_0 corresponds to the stress-intensity factor at 63.2 percentile probability of failure, and K_{min} represents the macroscopic threshold fracture toughness.

2.2 CMSG Fundamentals

The success of the microscopic Weibull stress model in predicting the probability of fracture predicates largely on the accuracy in computing the near-tip stress field. The classical plasticity fails to recognize the material hardening contributed by the gradient in the strain field when plastic deformations occurs in the micron or sub-micron levels, and thus may severely underestimate the near-tip stress fields. This under-estimation of the near-tip stress field by the classical plasticity theory leads potentially to lower Weibull stress values and subsequently under-predict probabilities of cleavage fracture.

To overcome the above, we implement the conventional mechanism-based strain gradient plasticity (CMSG) in computing the near-tip stresses to evaluate the scalar microscopic crack driving force, the Weibull stress, σ_w. The CMSG theory introduces an intrinsic length scale, l, in the constitutive relationship of the material. The flow stress, σ_f, is expressed as (Huang *et al*. 2001),

$$\sigma_f = \sigma_y \sqrt{f^2\left(\varepsilon^p\right) + l\eta^p}, \tag{5}$$

where σ_y defines the material yield strength, ε^p denotes the plastic strain, the function $f(\varepsilon^p)$ describes the uni-axial power-law hardening relationship and η^p represents the effective plastic strain gradient expressed as

$$\eta^p = \frac{\sqrt{\eta_{ijk}\eta_{ijk}}}{2}. \tag{6}$$

The third-order strain gradient tensor derives from the partial derivative of the second-order plastic strain tensor with respect to the spatial coordinate. Derivation details can be found in Swaddiwudhipong *et al*. (2006).

The power law visco-plastic model with strain gradient effects is expressed as,

$$\dot{\varepsilon}^p = \dot{\varepsilon}\left[\frac{\sigma_e}{\sigma_y \sqrt{f^2\left(\varepsilon^p\right) + l\eta^p}} \right]^n, \tag{7}$$

where n refers to the rate-sensitive coefficient and σ_e denotes the effective stress. The constitutive relation with the strain gradient effect is thus,

$$\dot{\sigma}'_{ij} = K\dot{\varepsilon}_{kk}\delta_{ij} + 2\mu\left\{\dot{\varepsilon}'_{ij} - \frac{3\dot{\varepsilon}}{2\sigma_e}\left[\frac{\sigma_e}{\sigma_y\sqrt{f^2\left(\varepsilon^p\right)+l\eta^p}}\right]^n \sigma'_{ij}\right\}, \tag{8}$$

where μ defines the shear modulus and K the bulk modulus.

The current study implements the CMSG formulation through a user-subroutine in ABAQUS finite element software (SIMULIA 2011) using elements with reduced integration. The analysis utilizes the C^0 20-node solid element with strain gradient material models described by the CMSG theory (Swaddiwudhipong *et al*. 2005).

2.3 Re-Calibration of the Weibull Parameters Based on CMSG Plasticity

The current study re-calibrates the Weibull modulus, m, and the threshold fracture toughness, K_{min}, for the 22-Ni-MoCr37 Euro steels, the experimental data of which are collected from a five-year European Union project (Heerens and Hellmann 2002). Figure 1 shows the typical finite element meshes used in the Weibull stress calculation for the calibration procedure, which is illustrated in detail by Wasiluk *et al*. (2006).

The FE meshes in Fig. 1 often contain an initial root radius of R_0 to facilitate the numerical convergence under large deformations. (Qian *et al*. 2011) have examined the effect of initial root radius in the calculation of the Weibull stress, and concluded that the variation of R_0 values from 0.002 μm and 10 μm does not impose significant effect on the values of Weibull stress in a small-scale yielding, modified boundary layer model.

Figure 2 compares the Weibull stresses computed from the classical plasticity and the CMSG plasticity for the small-scale yielding model and the compact tension, C(T), specimens, with a Weibull modulus of m = 10. The Weibull stresses calculated using the CMSG theory show significantly larger values than those based on the classical plasticity. The Weibull stresses computed using different intrinsic material length scales (l = 5 μm and l = 10 μm) indicate marginal differences as the load increases.

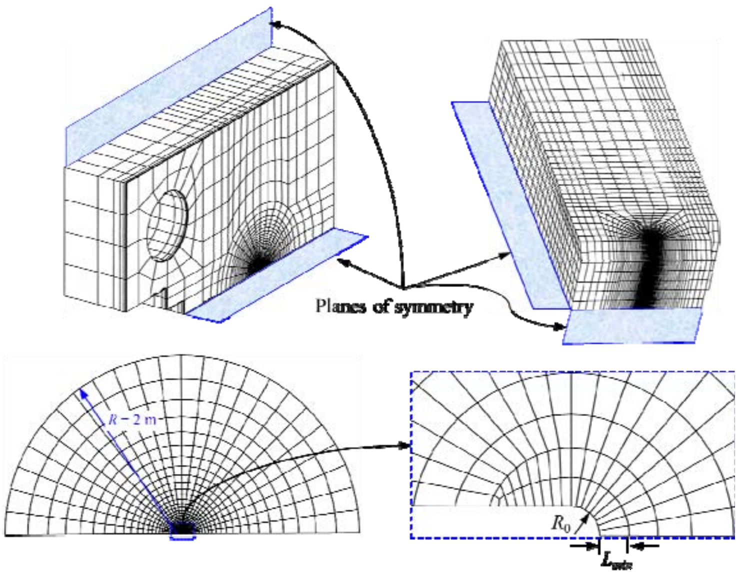

Fig. 1 Typical finite element models used in CMSG-based Weibull stress calculation.

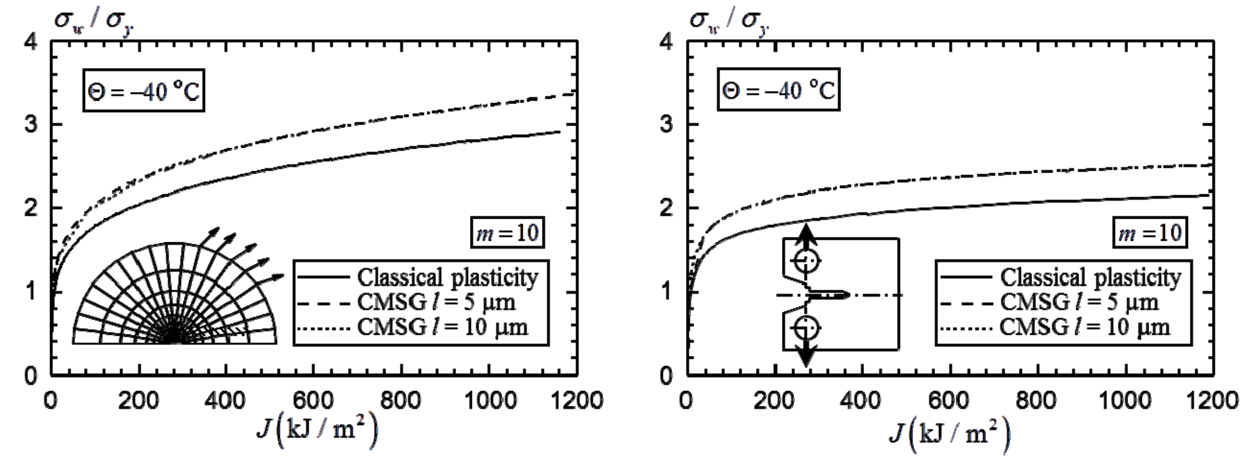

Fig. 2 Comparison of Weibull stresses based on classical and CMSG plasticity.

The calibration procedure outlined in (Wasiluk *et al*. 2006) requires two sets of experimental data to determine the Weibull shape parameter *m* and the threshold Weibull stress σ_{min}. The uniqueness of the two Weibull parameters (m and σ_{min}) requires the availability of two sets of experimental data with contrast differences in the crack-front constraints. The calibration criterion aims to determine the *m* and K_{min} values which minimize the following error function,

$$\mathrm{Error}\left(m, K_{min}\right) = \sum_{i=1}^{n_{\mathrm{LC}}+n_{\mathrm{HC}}} \left| K_{Jc(i)}^{x\mathrm{C-1T\,SSY}} - K_{Jc(i)}^{\mathrm{1T\,SSY}} \right| \mathrm{WF}_{(i)} + \sum_{i=1}^{\min\left(n_{LC}+n_{HC}\right)} \left| K_{Jc(i)}^{\mathrm{HC-1T\,SSY}} - K_{Jc(i)}^{\mathrm{LC-1T\,SSY}} \right| \mathrm{WF}_{(i)}, \tag{9}$$

3. OVER-NONLOCAL GRADIENT ENHANCED PLASTICITY DAMAGE MODEL FOR CONCRETE

3.1 Plasticity damage concrete model

In this contribution, we adopt the plasticity damage model for concrete developed by Grassl and Jirasek (2006). Numerical predictions from this model match experimental data reasonably well for a wide spectrum of loading conditions. We show the mesh sensitivity solutions during strain softening, as well as the partial regularization of standard gradient enhancement. The nominal stress is given by

$$\boldsymbol{\sigma} = \left(1-\omega\right)\overline{\boldsymbol{\sigma}} \tag{10}$$

where ω is a damage parameter, characterized with an internal damage variable κ_d

$$\omega = 1-\exp\left(-\kappa_d / \varepsilon_f\right) \quad , \quad \varepsilon_f \text{ = material parameter} \tag{11}$$

The model is implemented numerically in the FE software ABAQUS (SIMULIA 2011) using the material subroutine UMAT. We reproduce two numerical examples from Poh and Swaddiwudhipong (2009) to illustrate the versatility of the adopted model under different loading conditions (Figs 3 and 4).

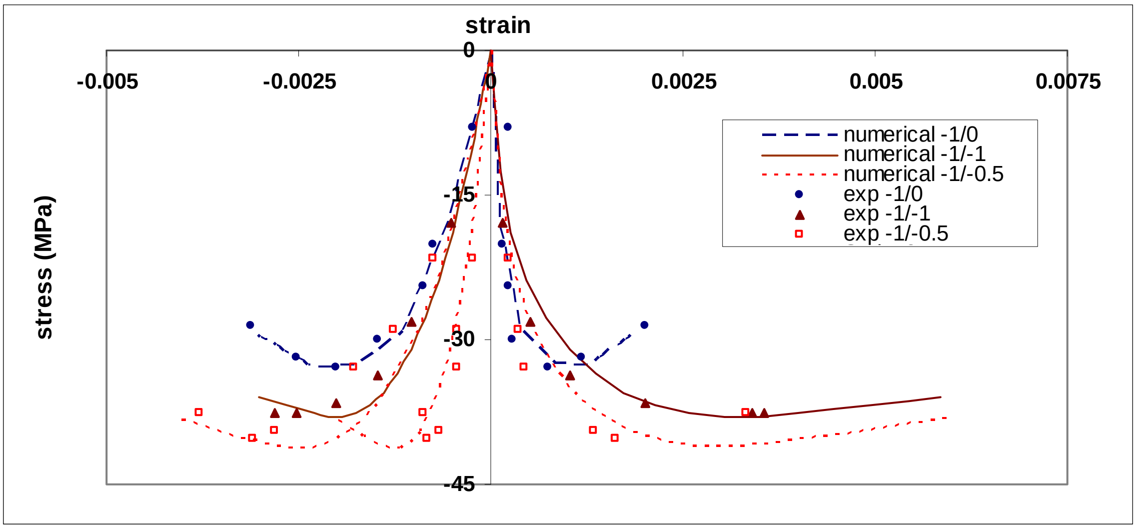

Fig. 3 Numerical solutions and experimental data in biaxial compression

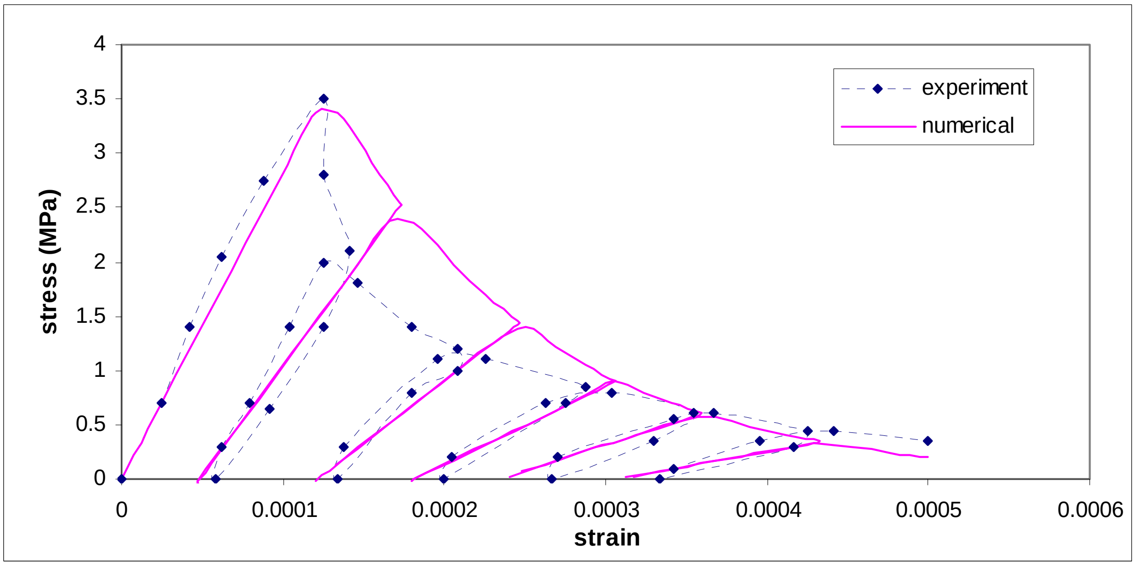

Fig. 4 Numerical solutions and experimental data in cyclical uniaxial tension

However, standard continuum models are inadequate during softening when a localization of deformation is induced by the loading conditions. This is illustrated with a double edge notch specimen in Fig. 5. During strain softening, the numerical solutions from the adopted model become strongly mesh dependent – the damaged region localizes to the smallest element size and orientation as shown in Fig. 6. Due to this pathological mesh dependency, the numerical predictions do not converge to a unique solution upon mesh refinement, see Fig. 7 – numerical solution becomes more brittle as the size of the element reduces.

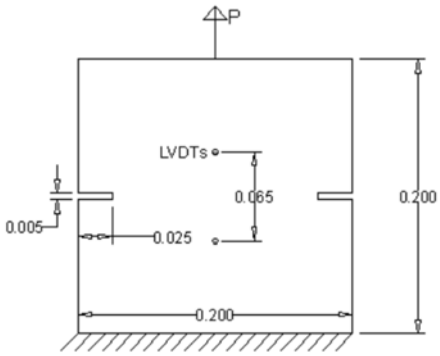

Fig. 5 Geometry (m) of a double edge notch specimen in uniaxial tension

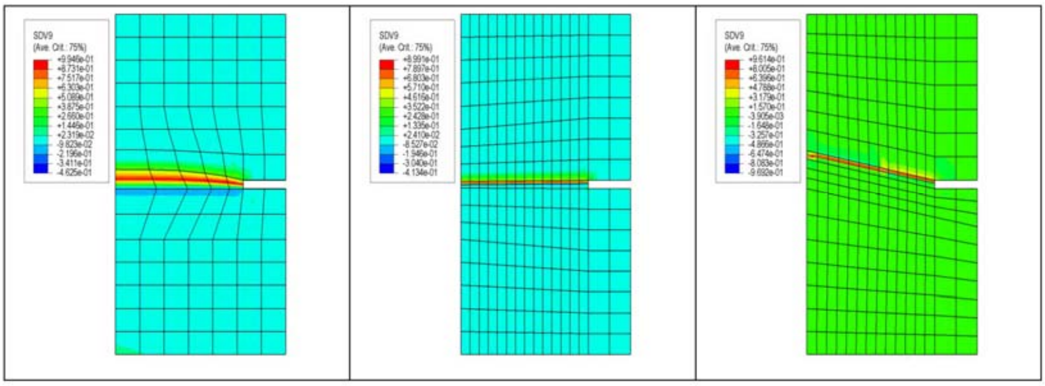

Fig. 6 Damage profiles for different mesh size and direction.

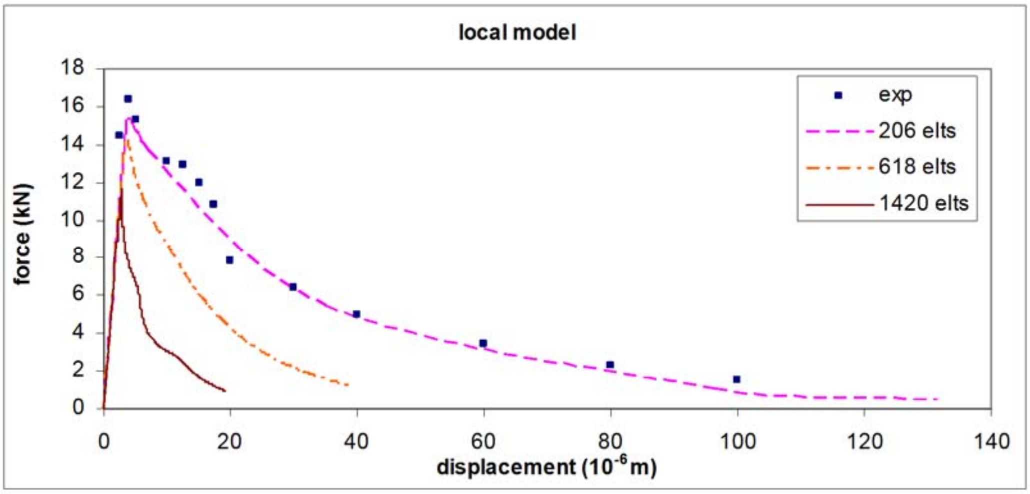

Fig. 7 Load displacement graphs for different mesh sizes.

3.2 Over-nonlocal gradient enhancement

To resolve the mesh dependency issue, a nonlocal enhancement is adopted. At a local point, the gradient enhancement requires information from its neighboring points, hence nonlocal. The standard gradient enhancement characterizes the damage process through the nonlocal internal damage variable $\bar{\kappa}_d$, given by

$$\bar{\kappa}_d(\mathbf{x}) - c\nabla^2\bar{\kappa}_d(\mathbf{x}) = \kappa_d(\mathbf{x}) \tag{12}$$

where c is a length scale parameter (units of length square) that characterizes the size of the damage micro-process region.

In the over-nonlocal formulation, the internal variable is taken as the weighted sum of the nonlocal and local values respectively, i.e.

$$\hat{\kappa}_d(\mathbf{x}) = m\bar{\kappa}_d(\mathbf{x}) + (1-m)\kappa_d(\mathbf{x}) \tag{13}$$

The weight for the nonlocal variable (m) is set greater than unity –hence over-nonlocal– and the excesses compensated by assigning a negative weight to the local component. Note that the standard gradient enhancement is recovered when $m = 1$. The nonlocal formulation is implemented numerically in ABAQUS via the user element subroutine UEL. Details are available in Poh and Swaddiwudhipong (2009) and not repeated here.

We consider again the double edge notch example with the gradient enhancement. The weight factor m is set close to unity ($m = 1.005$), so that it approaches the standard gradient enhancement. Numerical predictions from the gradient enhanced concrete model are shown in Fig. 8, a unique structural solution is now obtained during strain softening upon mesh refinement. Moreover, the model now predicts a consistent damage profile for different element sizes and orientations, as illustrated in Fig. 9. This demonstrates the ability of the over-nonlocal formulation to resolve the mesh dependency issues experienced by standard (local) continuum models.

The same problem is also solved with the standard gradient enhancement ($m = 1$). It can be shown that standard gradient enhancement produces a unique structural solution during softening. The structural response, shown in Fig. 10, is similar to the over-nonlocal enhancement ($m = 1.005$). However, with the standard implicit gradient model (m=1), deformation tends to localize into the smallest element, see Fig. 11. With the over-nonlocal enhancement (m=1.005), the crack propagates across the specimen width at failure, which is physically more correct.

This example thus shows that for certain models, although the structural response converges upon mesh refinements with the standard gradient enhancements, localization still occurs with discontinuous strain rates and the problem is only partially regularized. An over-nonlocal gradient enhancement, on the other hand, is able to fully regularize the softening response. It is also noted that just a slight increment from unity for the m parameter is able to induce full regularization during strain softening.

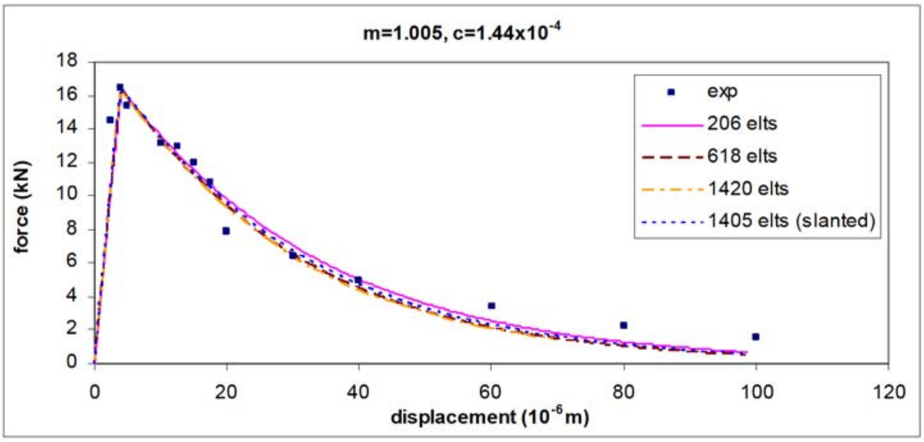

Fig. 8 Load displacement graphs with the over-nonlocal enhancement (m = 1.005)

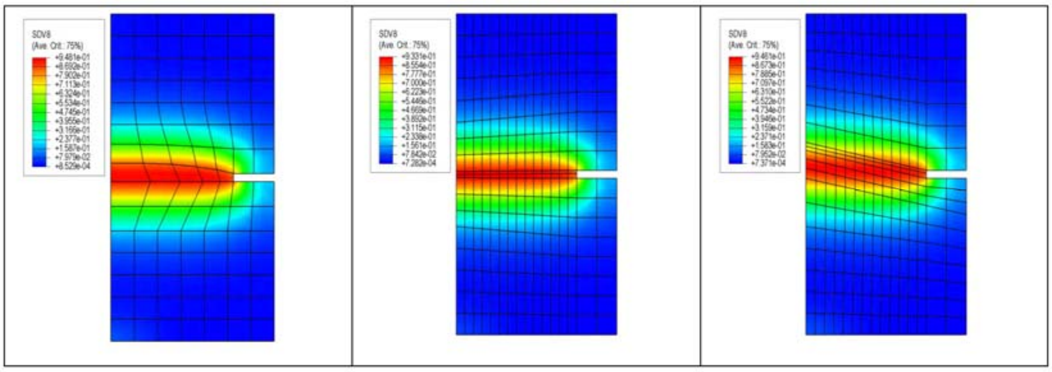

Fig. 9 Damage profiles for different mesh sizes and orientations (m = 1.005)

4. CONCLUSIONS

The values of Weibull stress and modulus incorporating CMSG plasticity deviate significantly from those of classical plasticity. The re-calibrated Weibull stress model can be used to predict fracture toughness probability distributions for the combined effects of constraint loss and crack front length statistics at the calibrated temperatures enabling the defect assessments in other practical applications based on the generated numerical results as well as available experimental datasets.

Local models exhibit strong mesh dependency during softening. Over-nonlocal gradient enhancement is a viable alternative when standard nonlocal formulation (m=1) fails to fully regularize the problem. The full regularization of solution through the over-nonlocal enhancement is demonstrated.

Comparison with analytical solutions and test results shows good agreement and reflects the necessity of including the effects of strain gradient plasticity in the formulation for non-uniform plastic deformation at small volume and over-nonlocal gradient enhancement on damaged model for solving problems involving materials with strain softening.

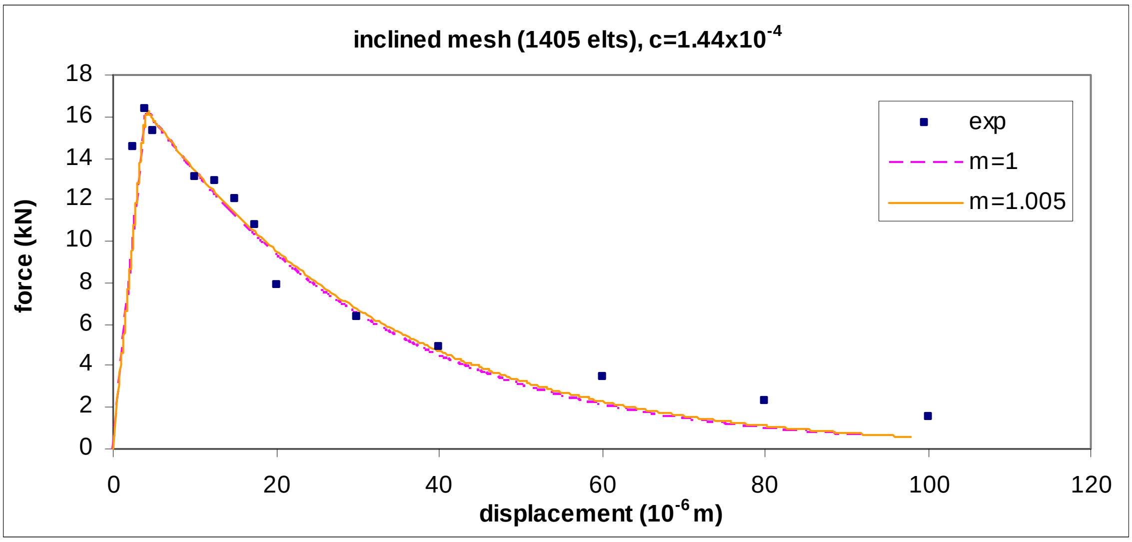

Fig. 10 Load displacement curves from standard gradient (*m* = 1) and over-nonlocal enhancements (*m*=1.005)

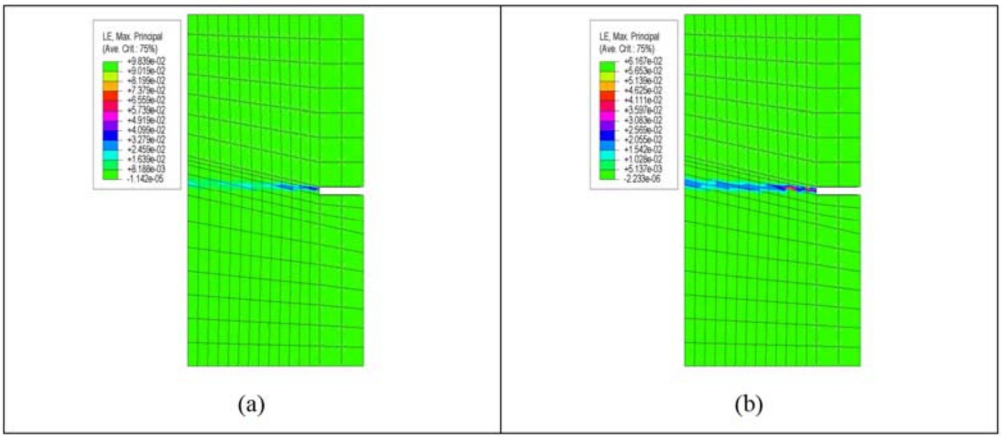

Fig. 11 Maximum principal strain for (a) *m* = 1 and (b) *m* = 1.005 respectively.

REFERENCES

American Society of Testing and Materials ASTM E-1921 (2012). *Standard test method for determination of reference temperature, T_0, for ferritic steels in the transition range*.

Beremin, F.M. (1983). "A local criterion for cleavage fracture of a nuclear pressure vessel steel". *Metall. Trans*., **14(A)**, 2277-2287.

Fleck, N.A., Muller, G.M., Ashby, M.F. and Hutchinson, J.W. (1994). "Strain gradient plasticity, theory and experiment". *Acta Metall. Mater.,* **42**, 475-487.

Grassl, P. and Jirásek, M. (2006). "Damage-plastic model for concrete failure". *Int. J. Solids Struct.*, **43**, 7166-7196.

Heerens, J. and Hellmann, D. (2002). “Development of the Euro fracture toughness dataset”. *Eng. Fract. Mech.*, **69**, 421-449.

Huang, Y., Qu, S., Hwang, K.C., Li, M. and Gao, H. (2004). “A conventional theory of mechanism-based strain gradient plasticity”. Int. J. Plasticity, **20**, 753-782.

Poh, L.H. and Swaddiwudhipong, S. (2009), “Over-nonlocal gradient enhanced plastic-damage model for concrete”. *Int. J. Solids Struct.,* **46**, 4369-4378.

Qian, X.D., Zhang, S.F. and Swaddiwudhipong, S. (2011), “Calibration of Weibull parameters using the conventional mechanism-based strain gradient plasticity”. *Eng. Fract. Mech.,* **78**, 1928-1944.

SIMULIA Inc. (2009). *ABAQUS User’s Manual*.

Stolken, J.S. and Evans, A.G. (1998), “A microbend test method for measuring the plasticity length scale”. *Acta Mater.*, **46**, 5109-5115.

Swaddiwudhipong, S., Hua, J., Tho, K.K. and Liu, Z.S. (2005), “C^0 solid elements for materials with strain gradient effects”. *Int. J. Numer. Meth. Eng.,* **64**, 1400-1414.

Swaddiwudhipong, S., Tho, K.K., Hua, J., Liu, Z.S. (2006), “Mechanism-based strain gradient plasticity in C^0 axisymmetric element”. *Int. J. Solids Struct.,* **43**, 1117-1130.

Wasiluk, B. Petti, J.P. and Dodds, R.H. Jr. (2006). “Temperature dependence of Weibull stress parameters: studies using the Euro-materials”. *Eng. Fract. Mech.* **73**, 1046-1069.